AP-1 and clathrin are essential for secretory granule biogenesis in *Drosophila*

Jason Burgess[a,b], Miluska Jauregui[a,b], Julie Tan[a,b], Janet Rollins[c], Sylvie Lallet[d,e], Peter A. Leventis[b], Gabrielle L. Boulianne[a,b], Henry C. Chang[f], Roland Le Borgne[d,e], Helmut Krämer[g], and Julie A. Brill[a,b]

[a]Department of Molecular Genetics, University of Toronto, Toronto, Ontario M5S 1A8, Canada; [b]Program in Developmental and Stem Cell Biology, The Hospital for Sick Children, Toronto, Ontario M5G 1L7, Canada; [c]Division of Natural Sciences, The College of Mount Saint Vincent, Riverdale, NY 10471; [d]CNRS, UMR 6061, Institut de Génétique et Développement de Rennes, F-35043 Rennes, France; [e]UEB, IFR 140, Faculté de Médecine, Université de Rennes 1, F-35043 Rennes, France; [f]Department of Biological Sciences, Purdue University, West Lafayette, IN 47907-2054; [g]Department of Neuroscience, University of Texas Southwestern Medical Center, Dallas, TX 75390-9111

ABSTRACT **Regulated secretion of hormones, digestive enzymes, and other biologically active molecules requires the formation of secretory granules. Clathrin and the clathrin adaptor protein complex 1 (AP-1) are necessary for maturation of exocrine, endocrine, and neuroendocrine secretory granules. However, the initial steps of secretory granule biogenesis are only minimally understood. Powerful genetic approaches available in the fruit fly *Drosophila melanogaster* were used to investigate the molecular pathway for biogenesis of the mucin-containing "glue granules" that form within epithelial cells of the third-instar larval salivary gland. Clathrin and AP-1 colocalize at the *trans*-Golgi network (TGN) and clathrin recruitment requires AP-1. Furthermore, clathrin and AP-1 colocalize with secretory cargo at the TGN and on immature granules. Finally, loss of clathrin or AP-1 leads to a profound block in secretory granule formation. These findings establish a novel role for AP-1– and clathrin-dependent trafficking in the biogenesis of mucin-containing secretory granules.**

Monitoring Editor
Anne Spang
University of Basel

Received: Jan 20, 2011
Revised: Mar 31, 2011
Accepted: Apr 7, 2011

This article was published online ahead of print in MBoC in Press (http://www.molbiolcell.org/cgi/doi/10.1091/mbc.E11-01-0054) on April 13, 2011.

J. B. and M. J. generated mosaic clones, performed immunostaining, and acquired fluorescence micrographs. J. T. analyzed Sgs transcripts. J. B. and J. R. prepared salivary glands for electron microscopy. J. B., H. C., S. L., and R.L.B. generated fluorescently tagged constructs and transgenic flies. S. L. and R.L.B. recombined *AP-47*$^{SHE\text{-}11}$ onto an FRT chromosome and generated anti–AP-1γ antibodies. P.A.L. and G.L.B. generated anti-LqfR antibodies. H. K. performed mosaic clone analysis and contributed to experimental design. J. B. and J.A.B conceived of the experiments and cowrote the manuscript. All authors commented on the manuscript.

Address correspondence to: Julie A. Brill (julie.brill@sickkids.ca).

Abbreviations used: AP, adaptor protein; AP-1, clathrin adaptor protein complex 1; AP-3, clathrin adaptor protein complex 3; AP-47, gene encoding *Drosophila* AP-1μ; Chc, clathrin heavy chain; DsRed, *Discosoma* species red fluorescent protein; ER, endoplasmic reticulum; GFP, monomeric enhanced green fluorescent protein; LqfR, Liquid facets-Related (*Drosophila* EpsinR); Lva, Lava lamp; mCherry, monomeric Cherry fluorescent protein; PBS, phosphate-buffered saline; RFP, monomeric red fluorescent protein; RT, reverse transcriptase; Sgs, salivary gland secretion; TEM, transmission electron microscopy; TGN, *trans*-Golgi network; UAS, upstream activating sequence; VFP, Venus fluorescent protein.

INTRODUCTION

Constitutive secretion of proteins and lipids from the *trans*-Golgi network (TGN) toward the cell surface is believed to operate in all cells. Constitutive secretion is characterized by the rapid deployment of newly synthesized cargo toward its final cellular destination. Specialized secretory cells such as endocrine, neuroendocrine, and exocrine cells contain an additional pathway termed the regulated secretory pathway. One hallmark of this pathway is the storage of regulated secretory proteins at high concentration in dense-core secretory granules that can be released in response to an external signal. How secreted proteins enter the regulated secretory pathway is a source of debate and may prove to be cargo and cell-type specific (Dikeakos and Reudelhuber, 2007). In the case of endocrine and neuroendocrine cells, sorting of secreted cargo is believed to be content driven, with selective aggregation of regulated secretory proteins at the TGN playing a major role in secretory granule biogenesis (Borgonovo *et al*., 2006).

Little is known about the coat proteins that might be required on the cytoplasmic face to promote budding of lumenal regulated secretory cargo from the TGN. Initial studies in AtT20 pituitary cells noted that condensing secretory products accumulate in dilated regions of the TGN that are coated with clathrin (Tooze and Tooze,

1986). Similarly, in β-cells treated with monensin to perturb intracellular trafficking, proinsulin accumulates in a clathrin-coated compartment related to the TGN (Orci *et al.*, 1984). These observations raise the possibility that the formation of regulated secretory granules might require clathrin at the TGN.

Coat proteins selectively incorporate cargo into vesicles and provide a scaffold for vesicle formation. Clathrin and its associated heterotetrameric adaptor proteins (APs) make up a major class of vesicular coats. APs bind to sorting motifs found in the cytoplasmic tails of membrane cargo and function as links between vesicular cargo and the clathrin lattice, although some AP-3 and AP-4 coats lack clathrin (Dell'Angelica *et al.*, 1999; Hirst *et al.*, 1999; Peden *et al.*, 2002, 2004; Bonifacino and Traub, 2003; Barois and Bakke, 2005). The four different AP complexes (AP-1–4) have distinct sites of action in the cell (Boehm and Bonifacino, 2001; Robinson, 2004). Of these, the AP-1 complex has perhaps the most diverse roles, acting at the TGN to promote constitutive secretion (Chi *et al.*, 2008), at the TGN and endosomes to sort mannose 6-phosphate receptors (Doray *et al.*, 2002; Hinners and Tooze, 2003; Waguri *et al.*, 2003), at recycling endosomes of polarized cells to sort basolateral proteins (Cancino *et al.*, 2007; Gravotta *et al.*, 2007; Deborde *et al.*, 2008), and at immature secretory granules of specialized secretory cells to retrieve missorted proteins (Arvan and Castle, 1998; Klumperman *et al.*, 1998; Dittie *et al.*, 1999; Molinete *et al.*, 2000; Morvan and Tooze, 2008). Indeed, a coat composed of clathrin and AP-1 is required for maturation and condensation of regulated secretory granules (Dittie *et al.*, 1997, 1999; Klumperman *et al.*, 1998). In contrast to granule maturation, the roles of AP-1 and clathrin in initial stages of secretory granule formation are less well established. AP-1 and clathrin were shown to be required for formation of Weibel-Palade bodies, secretory organelles that store the hemostatic protein von Willebrand factor (Lui-Roberts *et al.*, 2005). However, a dominant-negative clathrin construct did not interfere with insulin granule production in neuroendocrine cells, suggesting these granules form through a clathrin-independent mechanism (Molinete *et al.*, 2001). Thus it is not clear how general a role AP-1 and clathrin play in granule biogenesis.

The larval salivary gland in the fruit fly *Drosophila melanogaster* provides an excellent system for molecular genetic analysis of factors required for formation of regulated secretory granules. During the last half of third-instar larval development, prior to pupariation, salivary gland cells initiate production of mucin-type secretory granules termed "glue" granules (Beckendorf and Kafatos, 1976; Korge, 1977; Lehmann, 1996). These granules contain highly glycosylated mucin-type glue proteins that are required to adhere the pupal case to a solid substrate during metamorphosis (Fraenkel, 1952; Fraenkel and Brookes, 1953). Of the six known glue proteins (also called salivary gland secretion or Sgs proteins), Sgs1, Sgs3, and Sgs4 contain extended amino acid repeats that are likely sites of oligosaccharide linkage (Muskavitch and Hogness, 1982; Garfinkel *et al.*, 1983; Roth *et al.*, 1999; our unpublished observations). These proteins, which are synthesized in response to a low-titer pulse of the steroid hormone ecdysone at the mid–third-instar larval stage, are stored until an additional high-titer pulse of ecdysone promotes their release at the onset of pupariation (Boyd and Ashburner, 1977; Berendes and Ashburner, 1978; Biyasheva *et al.*, 2001).

Secreted mucin-type glycoproteins are ubiquitous in metazoans and serve important roles in animal physiology. Here we analyze the mechanism of mucin-type glue granule biogenesis in third-instar larval salivary gland cells. We show that AP-1 and clathrin localize to the TGN prior to glue production, colocalize with newly synthesized glue proteins during early stages of granule formation, and are found at later stages on maturing glue granules. Genetic disruption or knockdown of AP-1 subunits strongly reduces clathrin localization to the TGN. Moreover, AP-1 and clathrin are required for glue granule formation; loss of AP-1 causes glue cargo to accumulate at the TGN and in small, highly aberrant granules. Our results reveal a requirement for AP-1 and clathrin in the formation of mucin-type secretory granules.

RESULTS

Glue granule biogenesis is developmentally regulated

To develop a system in which regulated secretion could be genetically manipulated, we characterized the process of glue granule formation and maturation in third-instar larval salivary glands using a fluorescently tagged glue protein (Sgs3-DsRed) expressed under control of its own promoter (Biyasheva *et al.*, 2001; Costantino *et al.*, 2008). Glue expression was first visible in the distal-most cells of the salivary gland and proceeded proximally over time (Figure 1, A–C′), with the salivary gland increasing in size as glue production progressed. We defined the stages as 0 (no expression), 1 (small granules, expression in distal cells), and 2 (fully mature granules, expression in distal and proximal cells). Unlike glue protein, gamma-adaptin (AP-1γ), a large subunit of the AP-1 complex, was expressed in all cells of the salivary gland throughout third-instar larval development (Figure 1, A′–C′).

Glue granules exhibit several hallmarks of regulated secretory granules, including post-Golgi maturation and storage in the cytoplasm until an external stimulus triggers release. Sgs3-DsRed expression was undetectable prior to mid–third-instar (compare Figure 1, D and E). Accordingly, at stage 0, glue granules were not detected by transmission electron microscopy (TEM) (Figure 1G). At the onset of glue production (stage 1), small electron-dense glue granules were visible in the cytoplasm with an average diameter of 1.0 µm (Figure 1, E and H). Occasional L-shaped granules were also visible (Figure 1H), consistent with previous data suggesting growth by accretion (Farkas and Suakova, 1999). Between stages 1 and 2, glue granules increased in size (Figure 1, D–J) and electron-dense material became more prominent near the granule membrane (Figure 1I, arrowhead). During stage 2, fully mature glue granules reached an average diameter of 3.5 µm (Figure 1J). Following stage 2, glue granules fused with the apical membrane and glue cargo was secreted into the salivary gland lumen (Thomopoulos and Kastritis, 1979; Farkas and Sutakova, 1998; Biyasheva *et al.*, 2001; unpublished data).

To investigate the origin of glue granules, we used electron microscopy to analyze salivary glands in which glue granule production was just initiating. At the beginning of glue granule synthesis (stage 1), Golgi units composed of clusters of vesicles and tubules were present in close proximity to the rough endoplasmic reticulum (Thomopoulos *et al.*, 1992; Farkas and Sutakova, 1998; Kondylis *et al.*, 2001; Figure 1K). Small glue granules were visible in the cytoplasm adjacent to the Golgi complex. We also observed coated vesicles in the vicinity of the Golgi and early glue granules (Figure 1L). These ranged from 60 to 90 nm in diameter and were bristle-like in appearance, reminiscent of clathrin coats. The presence of small coated vesicles near the Golgi and developing glue granules suggested that granule formation might proceed via the formation of coated intermediate vesicles and consequently require coat proteins such as clathrin and its adaptors.

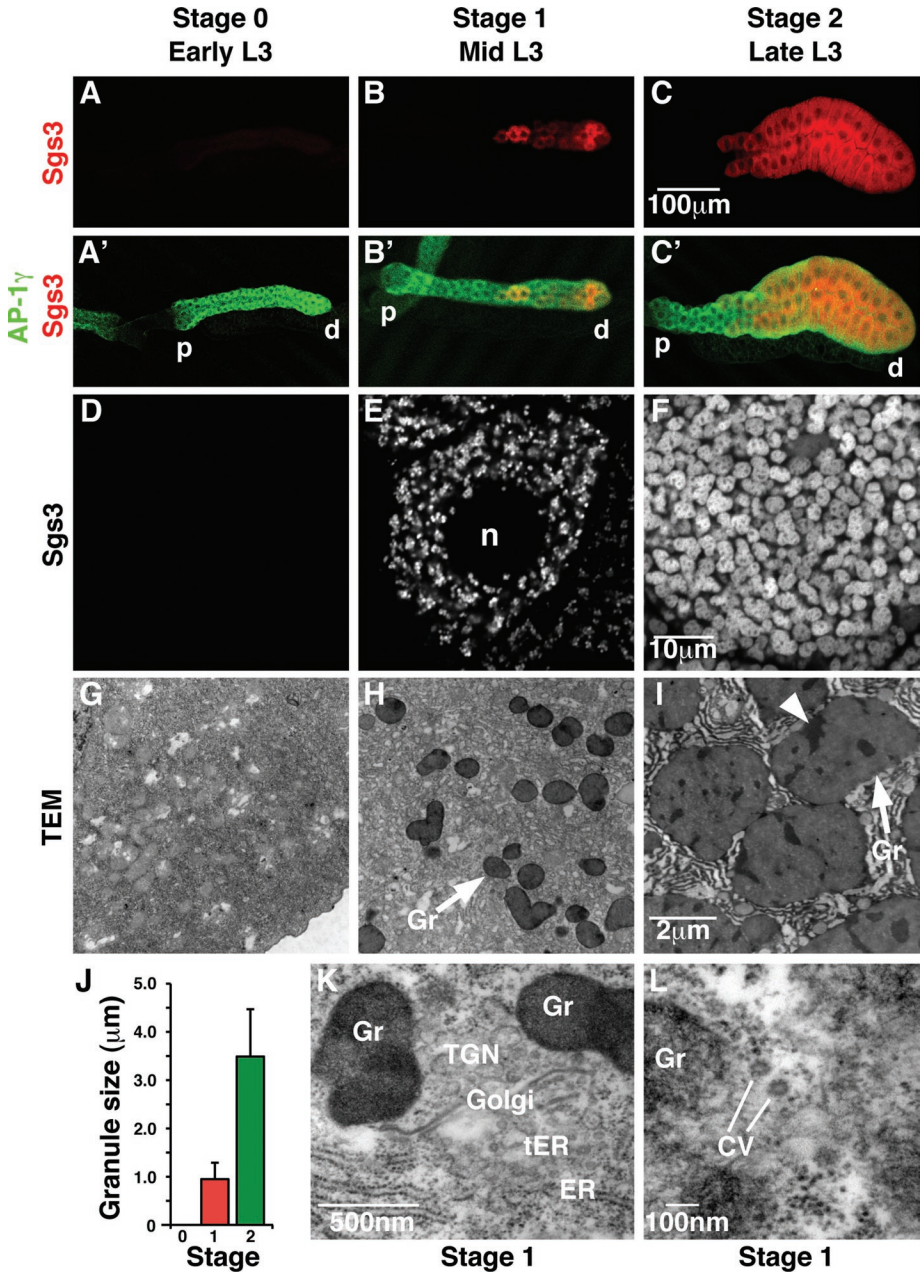

FIGURE 1: Glue granule biogenesis is developmentally regulated. (A–C′) Confocal micrographs of whole third-instar larval (L3) salivary glands expressing Sgs3-DsRed (red) and stained for AP-1γ (green), showing developmental timing of Sgs3-DsRed expression from stage 0 (no granules) through stage 1 (initiation of granule production) to stage 2 (fully mature granules or glands). AP-1γ is expressed in all cells of the salivary gland throughout development, whereas Sgs3-DsRed is first detected in distal (d) mid-L3 salivary gland cells (B, B′) and is expressed in more proximal (p) cells as development proceeds (C, C′). (D–F) Confocal micrographs of individual salivary gland cells showing developmental expression of Sgs3-DsRed. Sgs3-DsRed is not expressed in stage 0 (D). In stage 1, granules surround the nucleus (n) and appear uniformly small (E). In stage 2, granules are larger and occupy most of the cytoplasmic space (F). (G–I) Transmission electron micrographs (TEM) of L3 salivary glands staged using the Sgs3-DsRed marker. No granules were detected in stage 0 (G). Glue granule (Gr) maturation observed by TEM (H, I) parallels that seen by Sgs3-DsRed, validating this marker for following glue granule biogenesis (E, F). (J) Granules increase in size over time, from an average length of 1.0 μm ± 0.3 (n = 91) at stage 1 (red bar) to a maximum length of 3.5 μm ± 1.0 (n = 54) at stage 2 (green bar). (K, L) TEM of stage 1 salivary gland cells. Rough ER, transitional ER (tER), Golgi, and TGN (defined morphologically as in the work of Thomopoulos *et al.*, 1992; Kondylis and Rabouille, 2009) are present near small glue granules (Gr) (K). Coated vesicles (CV) were also observed near glue granules (Gr) (L).

Clathrin heavy chain and AP-1 localize to the *trans*-Golgi network

To identify coats that might function in granule biogenesis, we examined the subcellular distribution of clathrin heavy chain, as well as subunits of the clathrin adaptor protein complexes AP-1 and AP-3, which reside on intracellular organelles (note that *Drosophila* lacks AP-4; Boehm and Bonifacino, 2001). We first examined clathrin, AP-1, and AP-3 in salivary gland cells at stage 0, just prior to glue production. At this stage, Golgi bodies are easily visualized using antibodies directed against the golgin Lava lamp (Lva), which localizes to the *cis*-Golgi (Sisson *et al.*, 2000) (Figure 2, A–D″). Note that the *cis*-Golgi has a cup-shaped appearance. A monomeric red fluorescent protein fusion to clathrin heavy chain (RFP-Chc) predominantly localized to large puncta adjacent to the concave face of the *cis*-Golgi (Figure 2, A–A″), consistent with a previous report showing localization of endogenous Chc to intracellular puncta in these cells (Wingen *et al.*, 2009). Endogenous AP-1γ showed a similar distribution (Figure 2, B–B″). A projection constructed from serial confocal sections revealed numerous Golgi units scattered throughout the cytoplasm (Figure 2C). There was a one-to-one correspondence between AP-1γ– and Lva-positive structures, with the *cis*-Golgi cups surrounding AP-1γ in a manner consistent with AP-1 localizing to the TGN (Figure 2, C–C‴). Indeed AP-1γ and RFP-Chc colocalized with the *trans*-Golgi protein EpsinR (also called Liquid facets-Related or LqfR; Lee *et al.*, 2009) (Supplemental Figure S1A). In contrast, AP-1 showed only minimal overlap with the recycling endosome regulator Rab11 (Buszczak *et al.*, 2007; Lighthouse *et al.*, 2008) (Supplemental Figure S1B). AP-1γ and RFP-Chc colocalized at the TGN (Figure 2, D–D‴), although AP-1γ distribution appeared slightly more diffuse in salivary gland cells expressing RFP-Chc than in nonexpressing cells (compare Figure 2, B and D). Localization of AP-1 to the TGN is adaptor-protein specific, because a functional monomeric cherry fluorescent protein (mCherry) fusion to AP-3δ (called Garnet in *Drosophila*) showed no overlap with a Venus fluorescent protein (VFP) fusion to AP-1μ (called AP-47 in *Drosophila*) (Figure 2, E–E″), but rather colocalized with the late endosome marker Rab7 (unpublished data). Given the high degree of colocalization of clathrin and AP-1, we wondered whether AP-1 might be required to recruit clathrin to the TGN.

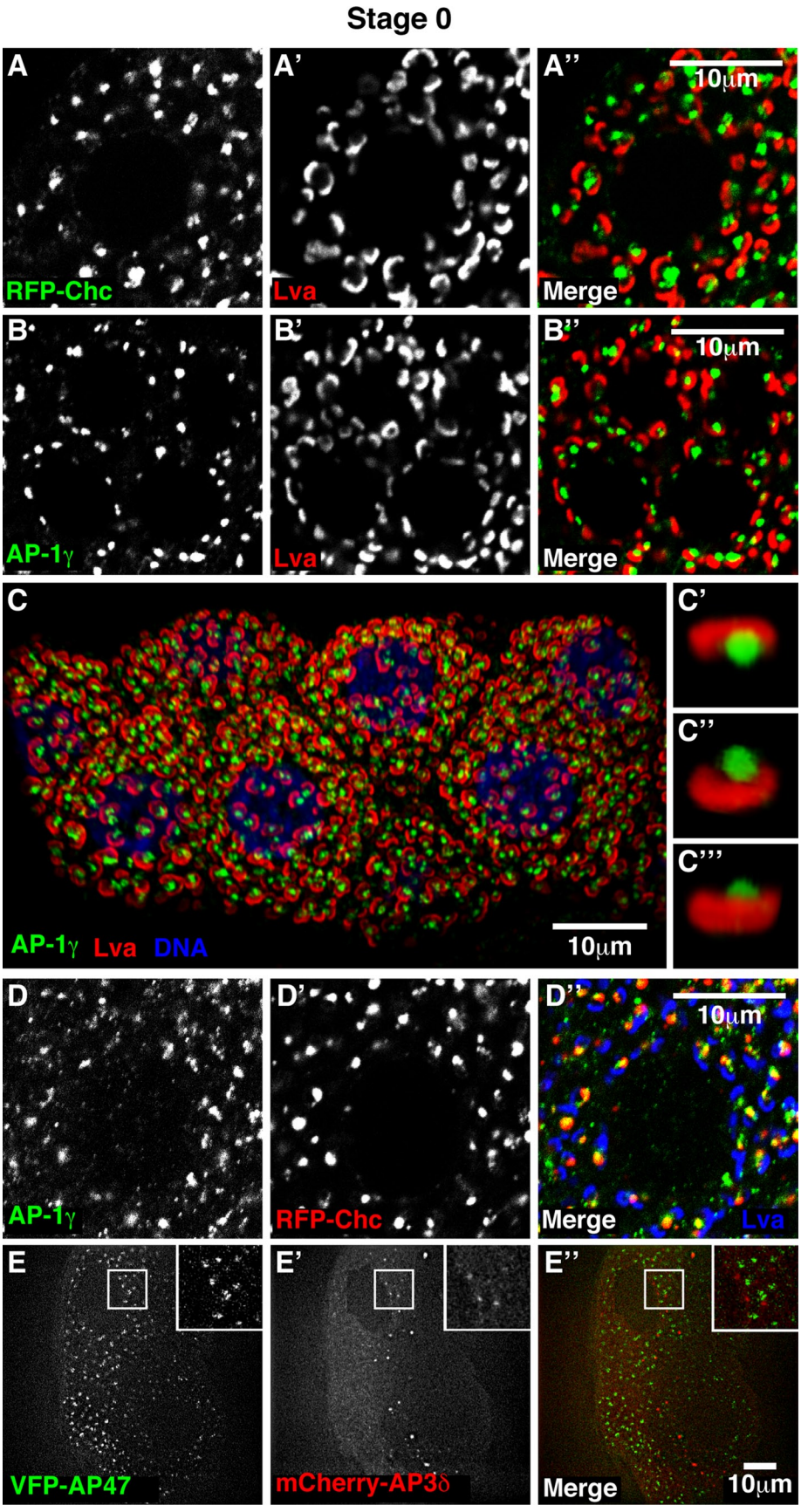

FIGURE 2: Clathrin heavy chain and the clathrin adaptor AP-1 colocalize at the *trans*-Golgi network. Confocal micrographs of stage 0 salivary gland cells. (A–A″) RFP-Chc (green) localizes adjacent to, but does not overlap with, the *cis*-Golgi marker Lva (red). (B–B″) Endogenous AP-1γ (green) localizes adjacent to Lva (red). (C–C‴) Projection of a series of spinning-disk confocal images of salivary gland cells stained for AP-1γ (green), Lva (red), and DNA (stained with DAPI; blue) reveals numerous Golgi bodies scattered throughout the cytoplasm (C). A three-dimensional rotation of a single Golgi body shows AP-1γ (green) adjacent to the cup-shaped Lva-positive *cis*-Golgi (red) (C′–C‴). Images were generated from Z stacks of 28 (C) or 5 (C′–C‴) optical sections acquired at a distance of 0.3 μm (see *Materials and Methods*). (D–D″) AP-1γ (green) and RFP-Chc (red) colocalize adjacent to Lva (blue). Colocalization of AP-1γ and RFP-Chc appears yellow in the merged image. (E–E″) Spinning-disk confocal images reveal that VFP-AP-47 (green) does not colocalize with mCherry-AP3δ (red). Boxed region is shown at 2× higher magnification in the insets.

AP-1 recruits clathrin to the *trans*-Golgi network

To test whether AP-1 recruits clathrin to the TGN, we made use of a μ1-adaptin null allele, *AP-47^{SHE-11}* (see *Materials and Methods*). To bypass late embryonic lethality caused by this allele, we generated mosaic clones in the salivary gland using FLP-FRT–based recombination (see *Materials and Methods*). Briefly, the wild-type chromosome carries a copy of green fluorescent protein (GFP) such that homozygous mutant cells are marked by the absence of GFP expression and heterozygous and wild-type cells are marked by one or two copies of GFP, respectively. *AP-47^{SHE-11}* clones were generated during embryogenesis and analyzed in third-instar larval salivary glands at stage 0, just prior to glue production. To determine whether other AP-1 subunits can localize to the TGN in the absence of AP-47, we examined the distribution of AP-1γ and found that its punctate localization was entirely lost in *AP-47^{SHE-11}* mutant cells (Figure 3, A–A″). Hence AP-47 is required for efficient recruitment or stability of AP-1γ, similar to what was previously observed in μ1-adaptin–deficient mouse embryonic fibroblasts (Meyer *et al.*, 2000). Not all trafficking markers were affected by the loss of AP-47, as the early endosome marker Rab5 was unperturbed (Figure 3, B–B″).

Strikingly, in *AP-47^{SHE-11}* mutant cells, RFP-Chc localization to the Golgi was dramatically reduced (Figure 3, C–C‴). The effect on RFP-Chc distribution was also observed in salivary gland cells in which expression of a double-stranded RNA was used to knock down expression of AP-1γ by RNA interference (RNAi) (Supplemental Figure S2). Most cells depleted of AP-1γ exhibited strong delocalization of RFP-Chc (compare Figure 3, D–D‴, with Figure 3, E–E‴), with only a few cells retaining weak RFP-Chc

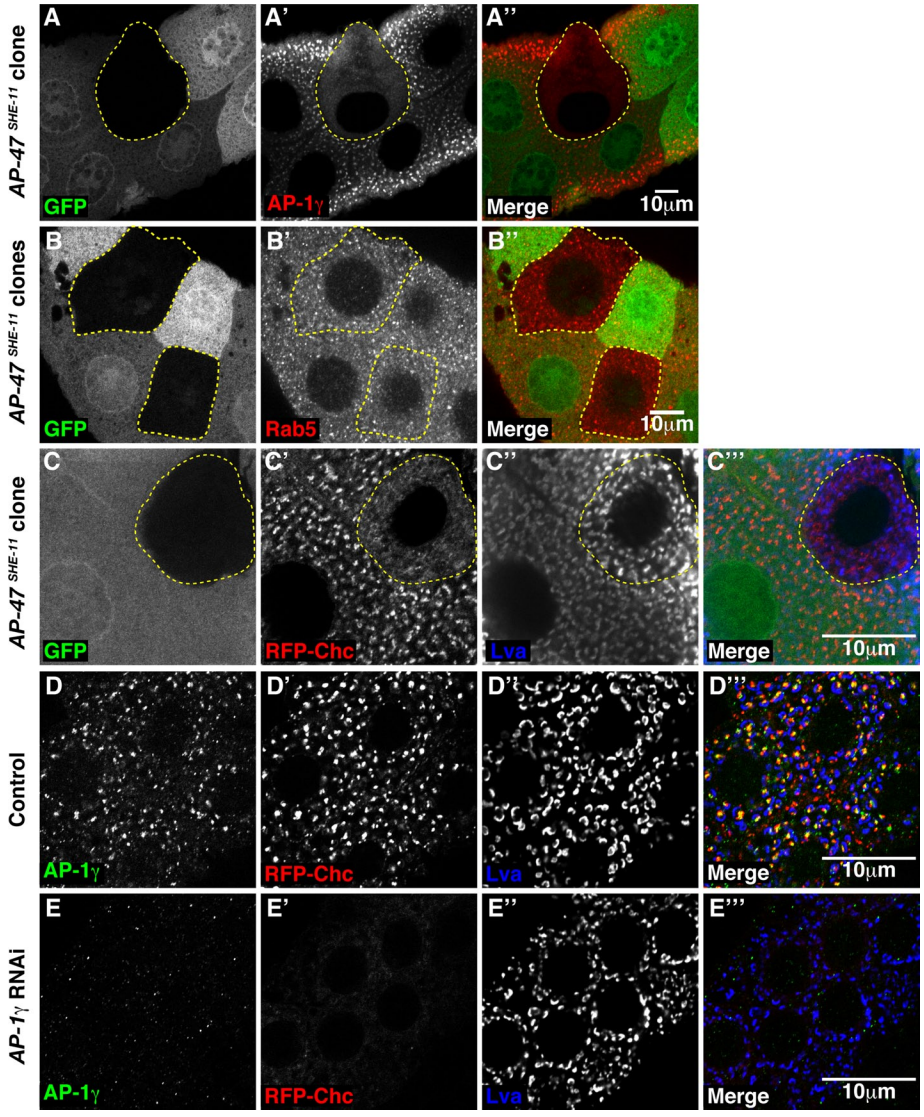

FIGURE 3: AP-1 is required to recruit clathrin to the *trans*-Golgi network. (A–C‴) Confocal micrographs of stage 0 salivary glands showing mutant clones (cells) marked by absence of GFP (green) and outlined in yellow. (A–A″) AP-1γ (red) localization is lost in an AP-1μ (*AP-47^{SHE-11}*) mutant cell. (B–B″) Rab5-positive early endosomes (red) are unaffected in *AP-47^{SHE-11}* mutant cells. (C–C‴) RFP-Chc (red) becomes largely cytoplasmic in an *AP-47^{SHE-11}* mutant cell, whereas the distribution of the *cis*-Golgi marker Lva (blue) is unaltered. Note that Lva shows a gradient of signal intensity due to incomplete antibody penetration of the tissue. (D–D‴) Control salivary gland cells expressing the *AB1-GAL4* driver alone show colocalization of AP-1γ (green) and RFP-Chc (red) adjacent to Lva (blue). (E–E″) Salivary gland cells expressing both the *AB1-GAL4* driver and a *UAS-AP-1γ* RNAi transgene are depleted of AP-1γ (green) and show cytosolic distribution of RFP-Chc (red), whereas Lva (blue) is largely unaffected. See also Supplemental Figure S2.

localization at the TGN (unpublished data). Hence the TGN is the major site of clathrin localization in these cells, and AP-1 plays a pivotal role in clathrin recruitment. Importantly, Golgi integrity per se (as assessed by distribution of Lva) was not affected by disruption of AP-1 (Figure 3, C″ and E″).

Newly synthesized glue proteins colocalize with AP-1 and clathrin at the TGN

Glue granule production is believed to follow the classical model of secretion, as outlined by Palade and coworkers, with secretory cargo being transported through the endoplasmic reticulum (ER) and Golgi prior to incorporation into secretory granules (Jamieson and Palade, 1967a, 1967b; Thomopoulos and Kastritis, 1979). To determine whether glue protein colocalizes with clathrin and/or AP-1, we analyzed Sgs3-DsRed localization in cells that had just switched on glue protein expression. In early stage 1, only a subset of the most distal salivary gland cells had initiated glue production (Figure 1B and Figure 4, A–A″ and B–B‴) and Sgs3-DsRed and AP-1γ partially colocalized adjacent to Lva, suggesting these proteins were at or near the TGN (Figure 4, A–A″). The association of glue-containing structures with AP-1 appeared to be transient, because some of the glue was also present in AP-1–negative puncta outside the Golgi (Figure 4, A–A″, yellow arrows). Importantly, Sgs3-DsRed colocalized with GFP-Chc as well as AP-1γ (Figure 4, B–B‴).

Later in stage 1, both GFP-Chc (Figure 4, C–C‴) and AP-1γ (Figure 4, D–D‴) associated with a subset of granules. Indeed, time-lapse fluorescence microscopy of live cells expressing VFP–AP-47 revealed that AP-1 localizes to the limiting membrane of a portion of small Sgs3-DsRed–containing granules (Supplemental Video 1). Moreover, small granules could be seen moving rapidly in the cytoplasm. Notably, granules exhibiting directed movement were not associated with AP-1, suggesting this coat must be shed for transport to occur. At stage 2, when granule biogenesis is nearly complete, GFP-Chc–positive puncta could still be seen. However, it was difficult to discern whether GFP-Chc localized to the limiting membrane of granules or to the cytoplasm adjacent to the granules (Figure 4, E–E″). In contrast to AP-1 and clathrin, AP3δ-GFP did not associate with stage 1 or stage 2 glue granules. Instead, AP3δ-GFP– and Rab7-positive late endosomes were located adjacent to the granules and became more prominent as granule biogenesis proceeded (compare Supplemental Figure S3, A–A″, with Supplemental Figure S3, B–B″; Rab7, not shown). The finding that AP-1 and clathrin are associated with glue cargo in the vicinity of the TGN and with post-Golgi glue granules suggested that these coat proteins might play a role in glue granule biogenesis.

AP-1 and clathrin are required for glue granule formation

To determine whether AP-1 is required for glue granule formation, we examined *AP-47^{SHE-11}* homozygous mutant cells in late–third-instar larvae, when glue granules are fully mature (stage 2). *AP-47^{SHE-11}* mutant cells either lacked detectible Sgs3-DsRed–containing glue granules (8 of 13 cells) (Figure 5, A–A″) or accumulated small granules in the cytoplasm (5 of 13 cells) (Figure 5, B–B″). This difference is likely due to variations in perdurance of AP-1μ protein in mutant cells. In addition, *AP-47^{SHE-11}* mutant cells also appeared smaller, suggesting that additional secretory

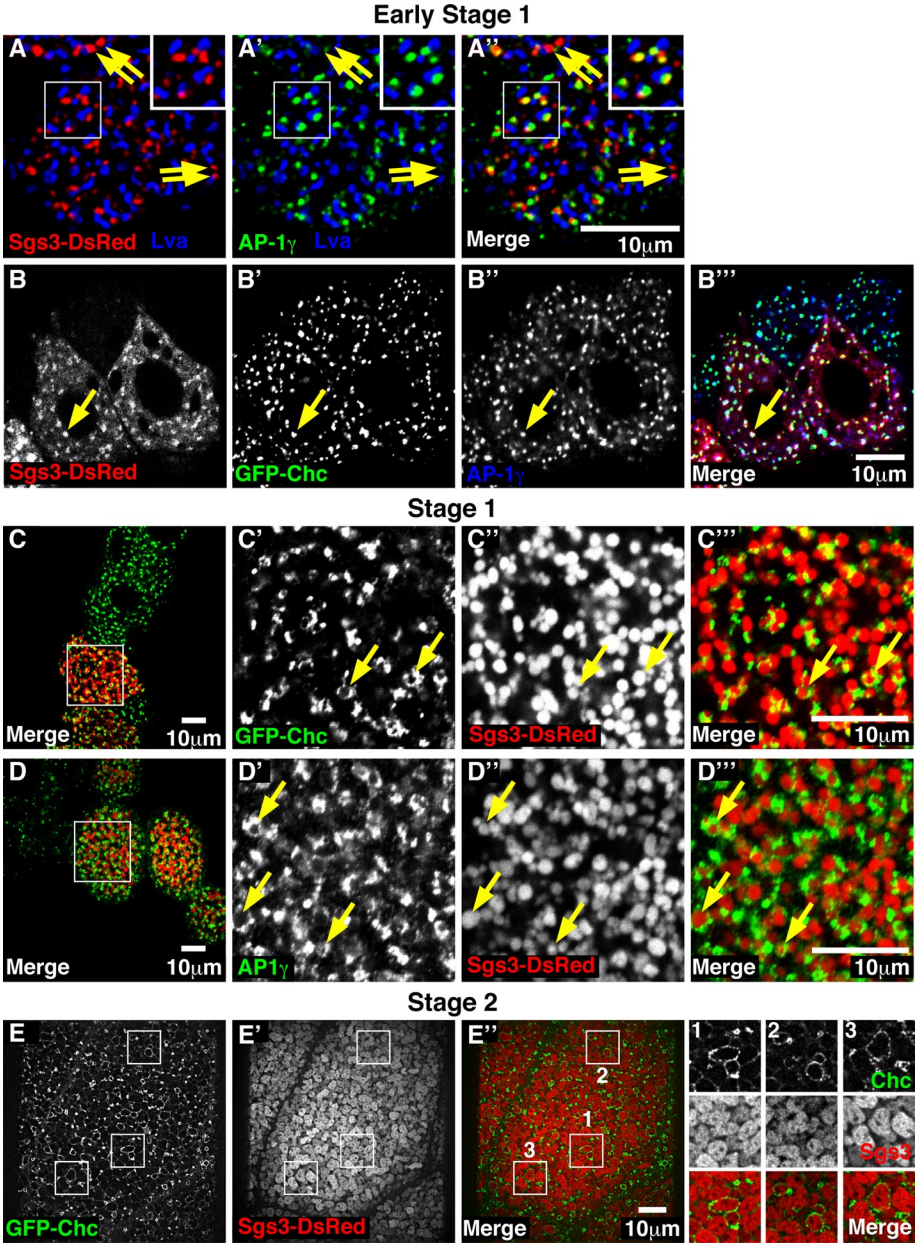

FIGURE 4: Sgs3-DsRed colocalizes with AP-1 and clathrin at the *trans*-Golgi network. Confocal fluorescence micrographs of third-instar salivary glands at the onset (early stage 1) (A–B‴), stage 1 (C–D‴), and stage 2 (E–E″) of glue production. (A–A″) Projections of a series of spinning-disk confocal images showing cells initiating Sgs3-DsRed (red) expression, stained with AP-1γ (green) and Lva (blue). In an early stage 1 cell, Sgs3-DsRed and AP-1γ partially colocalize (yellow) adjacent to the *cis*-Golgi marker Lva in a subset of Golgi bodies (A″). Boxed region is shown at 2× higher magnification in the insets. Note that a subset of the Sgs3-DsRed puncta does not colocalize with AP-1γ (yellow arrows). Images were generated from a Z stack of five optical sections acquired at a distance of 0.3 μm. (B–B‴) Sgs3-DsRed (red) partially colocalizes with both GFP-Chc (green) and AP-1γ (blue). Colocalization of Sgs3-DsRed with GFP-Chc and AP-1γ appears white in the merged image (B‴). (C–C‴) Low-magnification view of a portion of a salivary gland expressing GFP-Chc (green) and Sgs3-DsRed (red), showing a distal cell with a large number of stage 1 glue granules (C, boxed region; shown at higher magnification in C′–C‴). GFP-Chc partially coats a subset of Sgs3-DsRed–containing stage 1 glue granules (C′–C‴, yellow arrows). (D–D‴) Low-magnification view of a portion of a salivary gland stained for AP-1γ (green) and expressing Sgs3-DsRed (red) reveals numerous cells with stage 1 granules (D; boxed region is shown at higher magnification in D′–D‴). AP-1γ partially coats a subset of Sgs3-DsRed–containing granules (D′–D‴, yellow arrows). (E–E‴) Spinning-disk confocal micrographs of cells from a mature stage 2 salivary gland expressing GFP-Chc (green) and Sgs3-DsRed (red). GFP-Chc localizes near a broad range of Sgs3-DsRed–containing structures, including large stage 2 granules, as well as smaller vesicles (E″). Boxed regions 1–3 in E″ are shown at 2× higher magnification in the images on the right.

pathways involved in cell growth might be affected. Remarkably, AP-1μ showed dosage dependence, in that cells with only one wild-type copy of *AP-47* (marked by one copy of GFP) had intermediate-sized glue granules, whereas cells with two functional copies of *AP-47* (marked by two copies of GFP) had granules of normal size (Figure 5, A–A″). In support of the idea that AP-1 is limiting for granule biogenesis, third-instar larvae heterozygous for $AP\text{-}47^{SHE\text{-}11}$ and the hypomorphic allele $AP\text{-}47^{EP1112}$ were viable and exhibited glue granules of intermediate size (compare Figure 5, E and F).

Salivary gland cells in which AP-1γ was knocked down using RNAi were morphologically similar to $AP\text{-}47^{SHE\text{-}11}$ mutant cells; they either lacked detectible glue granules or accumulated very small granules (compare Figure 5, C and D). Because AP-1 is required to recruit clathrin to the TGN (Figure 3, C–C‴ and E–E″), we asked whether clathrin is also required for glue granule formation. The effect of depleting clathrin heavy chain by RNAi was even more dramatic than for AP-1, resulting in a complete block in glue granule formation in most cells, with only rare cells exhibiting small granules (Figure 5G). Consistent with a dramatic depletion of glue granules, pupal cases were poorly adherent to the vial wall and could easily be removed with a small paintbrush. These effects were specific to loss of AP-1 and clathrin, as mutations in *carmine* (cm^{1}) and *garnet* (g^{50e}), which encode the AP-3 subunits AP-3δ and AP-3μ, respectively, exhibited normal-sized glue granules (Figure 5, H and I).

To rule out an indirect effect of AP-1 on glue granule biogenesis, we tested whether glue gene transcripts were expressed at normal levels. Glue granule cargo consists of at least eight different proteins, all of which are highly expressed in the salivary gland during the third-instar larval stage. Semiquantitative reverse transcriptase–coupled PCR (RT-PCR) confirmed that AP-1γ transcripts were depleted in salivary glands in which AP-1γ had been knocked down by RNAi, whereas transcript abundance of a control gene, α-tubulin84B, was unaffected (Supplemental Figure S2, A and B). Interestingly, depletion of AP-1 had a moderate effect on glue gene expression. Levels of glue gene transcripts, including Sgs3-DsRed, were reduced by ~50% in AP-1γ knockdown glands as compared with controls. Importantly, glue gene transcription was still robustly initiated in salivary glands depleted of AP-1γ.

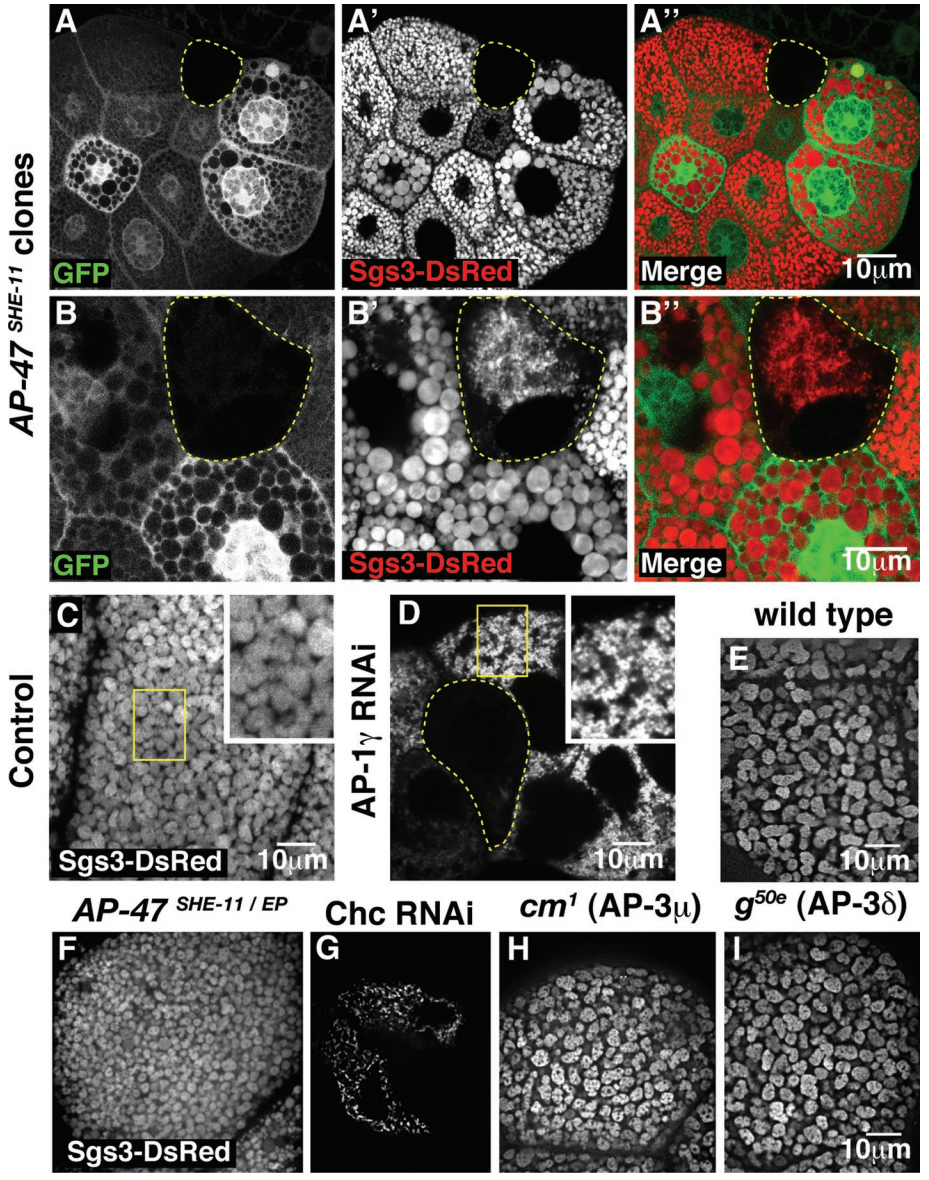

FIGURE 5: AP-1 is essential for glue granule biogenesis. Confocal fluorescence micrographs of late–third-instar (stage 2) larval salivary glands. (A–B″) AP-1μ (*AP-47*$^{SHE-11}$) mutant clones (cells marked by the absence of GFP (green) and outlined in yellow) exhibit a complete block in production of Sgs3-DsRed–containing glue granules (red) (A′ and A″) or strikingly small glue granules (B′ and B″). Note that cells with two copies of wild-type *AP-47* (marked by two copies of GFP) have larger granules than heterozygous cells (marked by one copy of GFP). (C–I) Confocal fluorescence micrographs of stage 2 larval salivary gland cells expressing Sgs3-DsRed. (C) Control salivary gland cells expressing the *AB1-GAL4* driver alone have granules of normal size (C, boxed region; shown at 2× higher magnification in inset). (D) Salivary gland cells expressing both the *AB1-GAL4* and a *UAS-AP-1γ* RNAi transgene completely lack glue granules (outlined cell) or have strikingly small glue granules (D, boxed region; shown at 2× higher magnification in inset). See also Supplemental Figure S2. (E–I) Spinning-disk confocal micrographs of salivary gland cells expressing Sgs3-DsRed. (E) Control wild-type cells showing normal-sized glue granules. (F) Larvae bearing the heteroallelic genotype *AP-47*$^{SHE-11/EP1112}$ exhibit intermediate-sized granules. (G) Depletion of clathrin heavy chain by RNAi in cells expressing *AB1-GAL4* and a *UAS-Chc* RNAi transgene causes a complete block in glue production in most cells, whereas a minority of cells produced small amounts of glue. (H and I) Strong loss-of-function mutations in AP-3μ (*carmine*^{1} [*cm*^{1}]) (H) or AP-3δ (*garnet*^{50e} [*g*^{50e}]) (I) have no effect on glue granule biogenesis.

Glue protein accumulates in aberrant vacuolated organelles in AP-1γ–depleted cells

To further define the fate of Sgs3-DsRed in AP-1γ–depleted cells, we assessed the localization of Sgs3-DsRed relative to the Golgi marker Lva. In wild-type stage 2 salivary gland cells, Lva-labeled Golgi bodies appeared scattered throughout the cytoplasm and were not tightly associated with mature granules containing Sgs3-DsRed (Figure 6, A–A″). In contrast, in AP-1γ–depleted salivary gland cells, glue protein showed an increased association with Lva-positive Golgi bodies (Figure 6, B–B″), and these appeared swollen relative to those in control cells (compare Figure 6, A and B). Indeed, the Golgi in AP-1γ knockdown cells more closely resembled those of cells prior to onset of glue production (compare Figure 2, A′ and B′, with Figure 6B). Notably, a similar increase in TGN volume was observed when post-Golgi secretion was blocked by incubation of kidney epithelial cells at moderately low temperatures (20°C) (Griffiths *et al.*, 1989; Ladinsky *et al.*, 2002). Sgs3-DsRed was also visible in post-Golgi structures most likely corresponding to abnormal immature granules (Figure 6, B′ and B″).

To determine the morphology of the Sgs3-DsRed–positive organelles in AP-1γ–depleted cells, we examined salivary glands by TEM. Numerous enlarged, vacuolated structures containing fibrillar cargo were visible throughout the cytoplasm (compare Figure 6, C and D). Notably, these structures did not resemble early glue granules observed in wild-type cells, clearly indicating an essential role for AP-1 in the formation of normal secretory granules.

DISCUSSION

We provide compelling evidence of a previously unknown function for clathrin and AP-1 in the formation of mucin-type secretory granules. We show that clathrin and AP-1 localize to the TGN prior to synthesis of secretory cargo, colocalize with newly synthesized secretory cargo, and are required for secretory granule formation. Hence AP-1 and clathrin play a crucial role in early stages of secretory granule formation in salivary gland cells. Consistent with this idea, clathrin becomes delocalized upon AP-1 depletion, indicating that other adaptors cannot recruit clathrin in the absence of AP-1 at this stage of salivary gland development.

Our results suggest that formation of mucin-containing glue granules and Weibel-Palade bodies might be similar. Weibel-Palade bodies have an unusual cigar-shaped appearance and it was proposed that AP-1 and clathrin might participate in their formation at the TGN by allowing lumenal cargo to properly fold and aggregate or by preventing premature scission (Lui-Roberts *et al.*, 2005; Metcalf *et al.*, 2008). Indeed, depletion of AP-1 in endothelial cells results in the formation of small, round von Willebrand factor–containing organelles lacking other

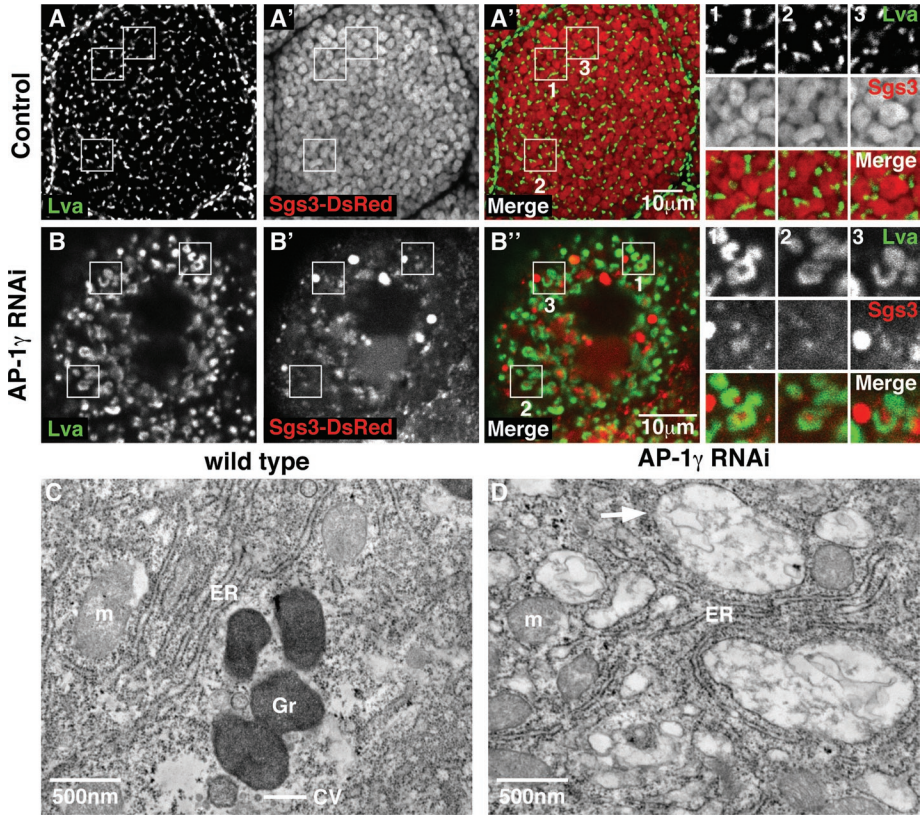

FIGURE 6: Glue protein accumulates at the *trans*-Golgi network and in aberrant vacuolated organelles in AP-1γ–depleted cells. (A–B") Confocal fluorescence micrographs of late–third-instar (stage 2) salivary glands expressing Sgs3-DsRed (red) and stained for the *cis*-Golgi marker Lva (green). Lva is distributed throughout the cytoplasm but is not associated with mature Sgs3-DsRed–containing granules in control cells expressing *AB1-GAL4* alone (A–A"; boxed regions 1–3 in A" are shown at 2× higher magnification in the images on the right). In cells expressing both the *AB1-GAL4* and a *UAS-AP-1γ* RNAi transgene, Sgs3-DsRed is associated with Lva-containing Golgi bodies and can also be seen in larger organelles (B–B"; boxed regions 1–3 in B" are shown at 2× higher magnification in the images on the right). (C and D) TEM of stage 1 salivary glands. Rough ER, mitochondria (m), nascent granules (Gr), and coated vesicles (CV) are visible in a wild-type cell (C). AP-1γ–depleted cells expressing both the *AB1-GAL4* and a *UAS-AP-1γ* RNAi transgene exhibit rough ER and mitochondria (m), as well as a large number of aberrant vacuolated organelles (D, white arrow). Micrograph is from a single experiment.

Weibel-Palade body markers. Our data demonstrate that the requirement for clathrin and AP-1 is not restricted to one specific type of granule. Depletion of clathrin or AP-1 in *Drosophila* salivary glands resulted in the accumulation of glue protein both at the TGN and in small organelles of aberrant morphology. This finding extends the role of AP-1 and clathrin to the formation of granules containing mucoprotein cargo and suggests a broader requirement for this coat complex in granule production.

How might AP-1 participate in glue granule formation? One possibility is that AP-1 and clathrin are directly involved in packaging glue granule cargo at the TGN. In mammalian cells, several transmembrane proteins are targeted to regulated secretory granules, including peptidyl-α-amidating monooxygenase, muclin, and phogrin (Bell-Parikh *et al.*, 2001; Wasmeier *et al.*, 2002; Boulatnikov and De Lisle, 2004; Dikeakos and Reudelhuber, 2007). Indeed, phogrin has been shown to bind to AP-1 and AP-2 through well-conserved tyrosine and dileucine sorting motifs present in its cytosolic tail (Torii *et al.*, 2005; Wasmeier *et al.*, 2005). How AP-1, a cytosolic coat protein, might interact with lumenal glue proteins in salivary cells remains to be determined. Because none of the known granule proteins contains a predicted transmembrane domain, a yet-unidentified transmembrane receptor might mediate this interaction.

A distinct possibility is that AP-1 might be required to maintain a steady-state distribution of proteins that shuttle between the TGN and endosomes such that they are available at the TGN during granule formation. For instance, the protein convertase furin recycles between the TGN and endosomes and is required to process numerous secreted proteins such as von Willebrand factor (Creemers *et al.*, 1993). Importantly, furin is no longer concentrated at the TGN in μ1A-deficient fibroblasts (Fölsch *et al.*, 2001). Thus failure to recycle transmembrane enzymes that play a crucial role in processing secreted cargo could also contribute to defective granule formation.

Reduced levels of AP-1 resulted in intermediate-sized granules, suggesting AP-1 might have an additional role during glue granule maturation. The development of *Drosophila* glue granules is characterized by an overall increase in size and decrease in number, consistent with homotypic fusion of smaller granules over time (Farkas and Suakova, 1999). Whether small and large granules are equally capable of fusing and whether fusion events are temporally regulated is not known. AP-1 might regulate granule maturation by sorting or retrieving membrane proteins required for homotypic fusion and eventual exocytosis. Additionally, AP-1 might function directly on maturing granules to remove missorted proteins, such as lysosomal hydrolases, similar to what has been reported for other types of secretory granules (Dittie *et al.*, 1996, 1997, 1999; Klumperman *et al.*, 1998). In support of this view, live imaging revealed a dynamic association of AP-1 with immature granules. Further studies are needed to resolve whether AP-1 functions in the addition and/or removal of proteins from maturing glue granules.

On the basis of the small size of mutant cells, AP-1 likely participates in additional trafficking pathways. In mammalian cells, AP-1A is ubiquitously expressed and required for trafficking between TGN and endosomes, whereas AP-1B is present only in polarized epithelial cells and is required for basolateral sorting from recycling endosomes (Fölsch *et al.*, 1999, 2001; Cancino *et al.*, 2007; Gravotta *et al.*, 2007; Deborde *et al.*, 2008). The sole AP-1 complex in *Drosophila* might mediate both functions in a single cell type. Interestingly, depletion of AP-1γ in salivary glands after granule formation caused the basolateral protein Discs large to redistribute to the apical surface (Peng *et al.*, 2009), suggesting that AP-1 is required for basolateral targeting of proteins in this tissue. However, an independent analysis of AP-1μ null cells in the dorsal thorax epithelium failed to reveal a similar polarity defect (Benhra *et al.*, 2011). This discrepancy might be due to cell type–specific requirements for AP-1 or to differences in RNAi versus mutant clones.

The observation that the abundance of Sgs3-DsRed protein and several Sgs mRNAs is reduced upon AP-1 knockdown suggests the existence of a negative-feedback loop, whereby a block in

anterograde secretory trafficking results in down-regulation of secretory genes. A block in secretion at the TGN could potentially induce the unfolded protein response, analogous to what happens upon depletion of the Arf1 GEF GBF1 (Citterio *et al.*, 2008). However, GBF1 functions early in the secretory pathway, and knockdown of two Arf-GEFs that act on the TGN did not elicit a similar response (Citterio *et al.*, 2008). Alternatively, a block in anterograde trafficking might repress transcriptional activation of secretory genes by *Drosophila* CrebA and Forkhead (Fkh) by some as-yet-unknown mechanism (Abrams and Andrew, 2005; Abrams *et al.*, 2006).

In addition to the AP-1 complex, the *Drosophila* genome encodes two other Golgi-localized clathrin adaptor proteins, EpsinR/LqfR and Golgi-localized, γ-ear–containing, ADP-ribosylation factor–binding (GGA) protein (*Drosophila* has only one GGA) (Hirst *et al.*, 2009; Lee *et al.*, 2009; Kametaka *et al.*, 2010). LqfR partially colocalizes with AP-1 at the TGN in salivary gland cells and *lqfR* mutants exhibit small salivary glands, suggesting defects in granule biogenesis (Lee *et al.*, 2009). It will be interesting to determine whether LqfR and GGA participate in glue granule biogenesis, especially since these clathrin adaptors might facilitate sorting of other types of cargo. For example, EpsinR has been shown to bind SNARE proteins and could function to provide vesicle identity to nascent glue-containing granules (Miller *et al.*, 2007; Chidambaram *et al.*, 2008). SNAP-24 was previously identified as a glue granule–specific SNARE, although whether this SNARE mediates homotypic fusion of granules or functions during exocytosis of granules at the plasma membrane is unclear (Niemeyer and Schwarz, 2000). Given the apparent similarities between glue granule and Weibel-Palade body biogenesis, as well as the high degree of conservation of TGN sorting machinery in *Drosophila*, our findings suggest that *Drosophila* salivary glands are of great utility to further elucidate the mechanisms of biogenesis of regulated secretory granules.

MATERIALS AND METHODS

Fly stocks and genetics crosses

Flies were raised on standard cornmeal molasses agar at 25°C (Ashburner, 1990). Visible markers and balancer chromosomes are as described (Lindsley and Zimm, 1992). *AP-47^{SHE-11}*, a deletion of amino acids 146–158 followed by a frameshift in the gene encoding the AP-1 subunit mu-adaptin, was isolated in a screen for modifiers of Presenilin-dependent Notch phenotypes (Mahoney *et al.*, 2006). *AP-47^{SHE-11}* was recombined onto *P{neoFRT}82B* to generate mosaic clones and to remove the second site *Psn^{143}* mutation (Xu and Rubin, 1993). *P{GawB}AB1-GAL4* and *P{w$^+$, Sgs3-GFP}* were obtained from the Bloomington *Drosophila* stock center. The *Rab11-GFP* protein trap line (CA07717), which carries a *piggyBack* transposon encoding EGFP inserted in frame with endogenous *Rab11* coding sequences, was obtained from A. Spradling (Buszczak *et al.*, 2007; Lighthouse *et al.*, 2008). Transgenic fly stocks carrying *P{w$^+$, UAS-mRFP-Chc}*, *P{w$^+$, UAS-EGFP-Chc}*, *P{w$^+$, αtub-mCherry-AP3δ}*, or *P{w$^+$, αtub-AP3δ-mEGFP}* (see later discussion) were generated by injection of *Drosophila* embryos using standard techniques. *P{w$^+$, Sgs3-DsRed}* flies were obtained from A. Andres (Costantino *et al.*, 2008). *P{w$^+$, UAS-AP-47::VFP}* flies were described previously (Benhra *et al.*, 2011). RNAi stocks expressing double-stranded RNAs under control of GAL4 upstream activating sequences (UASs) (Vienna *Drosophila* RNAi Center, Vienna, Austria; Dietzl *et al.*, 2007) were as follows: #3275 (*AP1γ*), #24017 (*AP1μ*), and #23666 (*Chc*). To examine salivary glands depleted of AP-1 or clathrin heavy chain, a stock carrying *Sgs3-DsRed*, *AB1-GAL4* was crossed to flies carrying the corresponding UAS-RNAi insertion.

Mosaic clones were generated using the FLP-FRT system (Golic and Lindquist, 1989) by crossing *y^1*, *w^{1118}*, *P{70FLP}3F;*; *P{neoFRT}82B*, *P{Ubi-GFP.D}83/TM6B*, *Hu*, *Tb* to flies containing *Sgs3-DsRed*; *P{neoFRT}82B*, *AP-47^{SHE-11}/TM6B*, *Hu*, *Tb*. To examine clathrin in *AP-47^{SHE-11}* clones, the heat shock FLP stock was crossed to *UAS-mRFP-Chc* / +; *P{neoFRT}82B*, *AP-47^{SHE-11}*, *AB1-GAL4/TM6B*, *Hu*, *Tb*. To generate mosaic clones in the salivary gland, adult flies were allowed to lay embryos in a vial during a 60-min collection window. Flies were then removed and embryos were aged for 2.5 h at room temperature. Embryos were then heat-shocked for 90 min at 37°C by placing the vial in a water bath. Embryos were then incubated at 25°C to allow for further development. Salivary gland cells (~100 per lobe) are specified early in embryonic development and differentiate without dividing (Campos-Ortega and Hartenstein, 1985). Consequently, mosaic clones generated in early embryos typically give rise to single-cell mutant clones.

Molecular biology

For Chc constructs, mRFP and EGFP were inserted in frame at the N-terminus of *Drosophila* Chc. For EGFP-Chc, an *Eco*RI-*Not*I fragment containing EGFP (without the stop codon) was first cloned into pUAST. pOT2-Chc, a plasmid containing the entire Chc ORF, was obtained from the *Drosophila* Genomics Research Center (Bloomington, IN). This plasmid contained a point mutation in Chc, which was repaired using the QuikChange Site-Directed Mutagenesis Kit (Strategene, Cedar Creek, TX). QuikChange was also used to introduce a *Not*I site before the ATG and a *Kpn*I site after the stop codon of Chc. After being verified by sequencing, the Chc ORF was cloned as a *Not*I-*Kpn*I fragment into pUAST-EGFP, resulting in pUAST-EGFP-Chc (GFP-Chc). pUAST-mRFP-Chc (RFP-Chc) was made in a similar manner. To generate mCherry-AP3δ and AP3δ-mEGFP (AP3δ-GFP), we used pCaSpeR-tub::mCherry, which contains an N-terminal mCherry (gift of R. Tsien; Shaner *et al.*, 2004) followed by an *Xba*I site, or pCaSpeR-tub::GFP, which contains a C-terminal mEGFP (gift of E. Snapp; Zacharias *et al.*, 2002) preceded by a *Kpn*I site. Both vectors are derived from a version of pCaSpeR4 (Pirrotta, 1988) containing the α-Tub84B promoter (gift of S. Eaton; Marois *et al.*, 2006). Restriction sites were introduced into a full-length *garnet* (RE06749) cDNA (Berkeley *Drosophila* Genome Project; obtained from the Canadian *Drosophila* Microarray Center, Mississauga, Canada) by PCR and orientation after subcloning was confirmed by DNA sequencing (The Center for Applied Genomics, SickKids, Toronto). AP3δ-GFP was fully functional in that it rescued the eye pigmentation defect of *garnet* mutant flies (J. B. and J. A. B., unpublished data).

RNA isolation and RT-PCR of salivary glands

To obtain salivary glands for RNA extraction, larvae were generated by crossing *w*; *Sgs3-DsRed*; *AB1-Gal4* virgin females to *UAS-AP1γ RNAi/TM6B, Hu, Tb* males. AP-1γ–depleted salivary glands were dissected from non-Tb larvae, and salivary glands from Tb siblings were used as controls. Ten pairs of salivary glands for each genotype were dissected and pooled in a microfuge tube containing 0.7% NaCl buffer; 600 μl of TRIzol (Invitrogen, Carlsbad, CA) was added, and tubes were centrifuged at 14,000 rpm for 1 min. Following addition of 120 μl of chloroform, the mixture was shaken vigorously by hand, incubated at room temperature for 3 min, and centrifuged at 14,000 rpm for 15 min at 4°C. The upper aqueous phase was transferred to a new microfuge tube, to which 0.7 volumes of isopropanol were added. RNA was left to precipitate overnight at −20°C, pelleted by centrifugation at 14,000 rpm for 30 min at 4°C, washed with 500 μl cold 70% ethanol, and dried by centrifugation in a SpeedVac (Thermo Scientific, Waltham, MA) for

5 min. The dry pellet was resuspended in 15 µl of diethylpyrocarbonate water and incubated for 15 min at 37°C.

cDNA libraries were generated from 1.7 µg of total salivary gland RNA using random decamers and the RETRO-SCRIPT reverse transcription kit (Ambion, Austin, TX) following manufacturer's recommendations for the two-step procedure. The linear range of PCR amplification was determined empirically, and PCR products of salivary gland cDNA were evaluated after 20 cycles. PCR primers for each transcript were designed to span one or more introns.

Fluorescence microscopy and imaging

Salivary glands from third-instar larvae were dissected in phosphate-buffered saline (PBS) (pH 7.4) and were either mounted and imaged directly in dissection buffer or fixed for 20 min on ice in PLP (4% paraformaldehyde, 0.01M sodium meta-periodate, 0.075 lysine, 0.035 phosphate buffer, pH 7.4). Fixed salivary glands were then washed once in PBS (pH 7.4) and permeabilized in PBST (PBS + 0.1% Triton X-100). Primary antibody incubation was performed overnight at 4°C in PBST with 5% normal goat serum. Salivary glands were mounted in PPD (0.1× PBS, 90% glycerol, 1 mg/ml *p*-phenylenediamine). Antibodies were used as follows: 1:1000 rabbit anti-Lva (gift of O. Papoulas and J. Sisson; Sisson *et al.*, 2000), 1:500 mouse anti-GFP monoclonal 3E6 (Invitrogen/Molecular Probes, Eugene, OR); 1:50 rabbit anti-Rab5 (gift of M. González-Gaitán; Wucherpfennig *et al.*, 2003), 1:500 mouse anti–AP-1γ (Benhra *et al.*, 2011), and 1:100 rabbit anti-LqfR (generated against a truncated protein lacking the Epsin N-terminal homology (ENTH) domain and shown to specifically recognize LqfR in immunoblotting and immunofluorescence experiments; P.A.L., G.L.B., J. B., and J.A.B., unpublished data). Anti-rabbit and anti-mouse secondary antibodies conjugated to Alexa-488, Alexa-568, or Alexa-633 were purchased from Molecular Probes (Invitrogen) and used as recommended by the manufacturer.

Fluorescence micrographs were acquired on a Zeiss LSM510 inverted laser scanning confocal microscope equipped with LSM objectives (20×, FLUAR NA 0.75; 40×, Plan-APOCHROMA NA 1.3; 63×, Plan-APOCHROMAT NA 1.4; or 100×, Plan-APOCHROMAT NA 1.4) and LSM510 software, or on a Quorum spinning-disk confocal microscope equipped with an SD 63× LCI Plan-NEOFLUAR 1.3 DIC Imm Kor (water) objective and Volocity acquisition software (SickKids Imaging Facility). Spinning-disk confocal images were deconvolved using the Iterative Restoration function of Volocity 4. Three-dimensional reconstructions were created using the three-dimensional opacity renderings of Volocity 4. All images were further processed for brightness and contrast levels using Adobe Photoshop CS2.

Electron microscopy

Salivary gland samples were prepared for TEM as previously described (Bazinet and Rollins, 2003). Salivary gland samples were staged using Sgs3-DsRed, which is expressed from endogenous promoter–enhancer elements, properly sorted into glue granules and secreted into the lumen in response to ecdysone (Biyasheva *et al.*, 2001). The presence of Sgs3-DsRed did not noticeably alter the appearance of mature granules by electron microscopy (unpublished data). Sections were viewed with a JEOL JTE 141011 microscope (SickKids/Mt. Sinai Advanced Center for Bioimaging). Images were obtained using AmtV542 acquisition software, and brightness and contrast were adjusted using Adobe Photoshop CS2.

ACKNOWLEDGMENTS

We thank members of the Brill lab for helpful discussions; John Ashkenas, Elizabeth Sztul, Lacramioara Fabian, Philip Goldbach, and Anya Cyprys for comments on the manuscript; Andrew Andres, Roger Tsien, Erik Snapp, Suzanne Eaton, Marcos González-Gaitán, Alan Spradling, Ophelia Papoulas, and the late John Sisson for flies, plasmids, and antibodies; Robert Temkin of The Hospital for Sick Children (SickKids)/Mt. Sinai Advanced Center for Bioimaging for technical assistance with electron microscopy; and Paul Paroutis of the Imaging Facility at SickKids for advice on confocal microscopy and image analysis. We are grateful for scholarships from NSERC and OGS (to J. B.); SickKids Restracomp funding (to J. T.); ARC No. 4905, Région Bretagne-ACOMB No. 2168, and the CNRS ATIP Program (to R.L.B.); The Welch Foundation (I-1300) and the NIH (EY-10199) to H. K.; an American Heart Association Scientist Development Grant and an American Cancer Society Research Scholar Grant (to H. C.); and grants from NSERC (262166) and The Cancer Research Society, Inc. (to J.A.B.).

REFERENCES

Abrams EW, Andrew DJ (2005). CrebA regulates secretory activity in the *Drosophila* salivary gland and epidermis. Development 132, 2743–2758.

Abrams EW, Mihoulides WK, Andrew DJ (2006). Fork head and Sage maintain a uniform and patent salivary gland lumen through regulation of two downstream target genes, PH4αSG1 and PH4αSG2. Development 133, 3517–3527.

Arvan P, Castle D (1998). Sorting and storage during secretory granule biogenesis: looking backward and looking forward. Biochem J 332 (Pt 3) 593–610.

Ashburner M (1990). *Drosophila*: A Laboratory Handbook, Cold Spring Harbor, NY: Cold Spring Harbor Laboratory.

Barois N, Bakke O (2005). The adaptor protein AP-4 as a component of the clathrin coat machinery: a morphological study. Biochem J 385, 503–510.

Bazinet C, Rollins JE (2003). *Rickettsia*-like mitochondrial motility in *Drosophila* spermiogenesis. Evol Dev 5, 379–385.

Beckendorf SK, Kafatos FC (1976). Differentiation in the salivary glands of *Drosophila melanogaster*: characterization of the glue proteins and their developmental appearance. Cell 9, 365–373.

Bell-Parikh LC, Eipper BA, Mains RE (2001). Response of an integral granule membrane protein to changes in pH. J Biol Chem 276, 29854–29863.

Benhra N, Lallet S, Cotton M, Le Bras S, Dussert A, Le Borgne R (2011). AP-1 controls the trafficking of Notch and Sanpodo toward E-cadherin junctions in sensory organ precursors. Curr Biol 21, 87–95.

Berendes HD, Ashburner M (1978). The salivary glands. In: The Genetics and Biology of *Drosophila*. Vol. 2b, ed. M Ashburner and TRF Wright, London and New York: Academic Press, 453–498 .

Biyasheva A, Do TV, Lu Y, Vaskova M, Andres AJ (2001). Glue secretion in the *Drosophila* salivary gland: a model for steroid-regulated exocytosis. Dev Biol 231, 234–251.

Boehm M, Bonifacino JS (2001). Adaptins: the final recount. Mol Biol Cell 12, 2907–2920.

Bonifacino JS, Traub LM (2003). Signals for sorting of transmembrane proteins to endosomes and lysosomes. Annu Rev Biochem 72, 395–447.

Borgonovo B, Ouwendijk J, Solimena M (2006). Biogenesis of secretory granules. Curr Opin Cell Biol 18, 365–370.

Boulatnikov I, De Lisle RC (2004). Binding of the Golgi sorting receptor muclin to pancreatic zymogens through sulfated O-linked oligosaccharides. J Biol Chem 279, 40918–40926.

Boyd M, Ashburner M (1977). The hormonal control of salivary gland secretion in *Drosophila melanogaster*: studies *in vitro*. J Insect Physiol 23, 517–523.

Buszczak M *et al.* (2007). The carnegie protein trap library: a versatile tool for *Drosophila* developmental studies. Genetics 175, 1505–1531.

Campos-Ortega JA, Hartenstein V (1985). The Embryonic Development of *Drosophila melanogaster*, Berlin and New York: Springer-Verlag.

Cancino J, Torrealba C, Soza A, Yuseff MI, Gravotta D, Henklein P, Rodriguez-Boulan E, Gonzalez A (2007). Antibody to AP1B adaptor blocks biosynthetic and recycling routes of basolateral proteins at recycling endosomes. Mol Biol Cell 18, 4872–4884.

Chi S, Cao H, Chen J, McNiven MA (2008). Eps15 mediates vesicle trafficking from the *trans*-Golgi network via an interaction with the clathrin adaptor AP-1. Mol Biol Cell 19, 3564–3575.

Chidambaram S, Zimmermann J, von Mollard GF (2008). ENTH domain proteins are cargo adaptors for multiple SNARE proteins at the TGN endosome. J Cell Sci 121, 329–338.
Citterio C, Vichi A, Pacheco-Rodriguez G, Aponte AM, Moss J, Vaughan M (2008). Unfolded protein response and cell death after depletion of brefeldin A-inhibited guanine nucleotide-exchange protein GBF1. Proc Natl Acad Sci USA 105, 2877–2882.
Costantino BF, Bricker DK, Alexandre K, Shen K, Merriam JR, Antoniewski C, Callender JL, Henrich VC, Presente A, Andres AJ (2008). A novel ecdysone receptor mediates steroid-regulated developmental events during the mid-third instar of *Drosophila*. PLoS Genet 4, e1000102.
Creemers JW, Siezen RJ, Roebroek AJ, Ayoubi TA, Huylebroeck D, Van de Ven WJ (1993). Modulation of furin-mediated proprotein processing activity by site-directed mutagenesis. J Biol Chem 268, 21826–21834.
Deborde S, Perret E, Gravotta D, Deora A, Salvarezza S, Schreiner R, Rodriguez-Boulan E (2008). Clathrin is a key regulator of basolateral polarity. Nature 452, 719–723.
Dell'Angelica EC, Mullins C, Bonifacino JS (1999). AP-4, a novel protein complex related to clathrin adaptors. J Biol Chem 274, 7278–7285.
Dietzl G *et al*. (2007). A genome-wide transgenic RNAi library for conditional gene inactivation in *Drosophila*. Nature 448, 151–156.
Dikeakos JD, Reudelhuber TL (2007). Sending proteins to dense core secretory granules: still a lot to sort out. J Cell Biol 177, 191–196.
Dittie AS, Hajibagheri N, Tooze SA (1996). The AP-1 adaptor complex binds to immature secretory granules from PC12 cells, and is regulated by ADP-ribosylation factor. J Cell Biol 132, 523–536.
Dittie AS, Klumperman J, Tooze SA (1999). Differential distribution of mannose-6-phosphate receptors and furin in immature secretory granules. J Cell Sci 112 (Pt 22), 3955–3966.
Dittie AS, Thomas L, Thomas G, Tooze SA (1997). Interaction of furin in immature secretory granules from neuroendocrine cells with the AP-1 adaptor complex is modulated by casein kinase II phosphorylation. EMBO J 16, 4859–4870.
Doray B, Ghosh P, Griffith J, Geuze HJ, Kornfeld S (2002). Cooperation of GGAs and AP-1 in packaging MPRs at the *trans*-Golgi network. Science 297, 1700–1703.
Farkas R, Suakova G (1999). Developmental regulation of granule size and numbers in larval salivary glands of *Drosophila* by steroid hormone ecdysone. Cell Biol Int 23, 671–676.
Farkas R, Sutakova G (1998). Ultrastructural changes of *Drosophila* larval and prepupal salivary glands cultured in vitro with ecdysone. In Vitro Cell Dev Biol Anim 34, 813–823.
Fölsch H, Ohno H, Bonifacino JS, Mellman I (1999). A novel clathrin adaptor complex mediates basolateral targeting in polarized epithelial cells. Cell 99, 189–198.
Fölsch H, Pypaert M, Schu P, Mellman I (2001). Distribution and function of AP-1 clathrin adaptor complexes in polarized epithelial cells. J Cell Biol 152, 595–606.
Fraenkel G (1952). A function of the salivary glands of the larvae of *Drosophila* and other flies. Biol Bull 103, 285–286.
Fraenkel G, Brookes VJ (1953). The process by which the puparia of many species of flies become fixed to a substrate. Biol Bull 105, 442–449.
Garfinkel MD, Pruitt RE, Meyerowitz EM (1983). DNA sequences, gene regulation and modular protein evolution in the *Drosophila* 68C glue gene cluster. J Mol Biol 168, 765–789.
Golic KG, Lindquist S (1989). The FLP recombinase of yeast catalyzes site-specific recombination in the *Drosophila* genome. Cell 59, 499–509.
Gravotta D, Deora A, Perret E, Oyanadel C, Soza A, Schreiner R, Gonzalez A, Rodriguez-Boulan E (2007). AP1B sorts basolateral proteins in recycling and biosynthetic routes of MDCK cells. Proc Natl Acad Sci USA 104, 1564–1569.
Griffiths G, Fuller SD, Back R, Hollinshead M, Pfeiffer S, Simons K (1989). The dynamic nature of the Golgi complex. J Cell Biol 108, 277–297.
Hinners I, Tooze SA (2003). Changing directions: clathrin-mediated transport between the Golgi and endosomes. J Cell Sci 116, 763–771.
Hirst J, Bright NA, Rous B, Robinson MS (1999). Characterization of a fourth adaptor-related protein complex. Mol Biol Cell 10, 2787–2802.
Hirst J, Sahlender DA, Choma M, Sinka R, Harbour ME, Parkinson M, Robinson MS (2009). Spatial and functional relationship of GGAs and AP-1 in *Drosophila* and HeLa cells. Traffic 10, 1696–1710.
Jamieson JD, Palade GE (1967a). Intracellular transport of secretory proteins in the pancreatic exocrine cell. I. Role of the peripheral elements of the Golgi complex. J Cell Biol 34, 577–596.
Jamieson JD, Palade GE (1967b). Intracellular transport of secretory proteins in the pancreatic exocrine cell. II. Transport to condensing vacuoles and zymogen granules. J Cell Biol 34, 597–615.
Kametaka S, Sawada N, Bonifacino JS, Waguri S (2010). Functional characterization of protein-sorting machineries at the *trans*-Golgi network in *Drosophila melanogaster*. J Cell Sci 123, 460–471.
Klumperman J, Kuliawat R, Griffith JM, Geuze HJ, Arvan P (1998). Mannose 6-phosphate receptors are sorted from immature secretory granules via adaptor protein AP-1, clathrin, and syntaxin 6-positive vesicles. J Cell Biol 141, 359–371.
Kondylis V, Goulding SE, Dunne JC, Rabouille C (2001). Biogenesis of Golgi stacks in imaginal discs of *Drosophila melanogaster*. Mol Biol Cell 12, 2308–2327.
Kondylis V, Rabouille C (2009). The Golgi apparatus: lessons from *Drosophila*. FEBS Lett 583, 3827–3838.
Korge G (1977). Larval saliva in *Drosophila melanogaster*: production, composition, and relationship to chromosome puffs. Dev Biol 58, 339–355.
Ladinsky MS, Wu CC, McIntosh S, McIntosh JR, Howell KE (2002). Structure of the Golgi and distribution of reporter molecules at 20 degrees C reveals the complexity of the exit compartments. Mol Biol Cell 13, 2810–2825.
Lee JH, Overstreet E, Fitch E, Fleenor S, Fischer JA (2009). *Drosophila liquid facets-Related* encodes Golgi epsin and is an essential gene required for cell proliferation, growth, and patterning. Dev Biol 331, 1–13.
Lehmann M *et al*. (1996). *Drosophila Sgs* genes: stage and tissue specificity of hormone responsiveness. Bioessays 18, 47–54.
Lighthouse DV, Buszczak M, Spradling AC (2008). New components of the *Drosophila* fusome suggest it plays novel roles in signaling and transport. Dev Biol 317, 59–71.
Lindsley DL, Zimm GG (1992). The Genome of *Drosophila melanogaster*, San Diego, CA: Academic Press.
Lui-Roberts WW, Collinson LM, Hewlett LJ, Michaux G, Cutler DF (2005). An AP-1/clathrin coat plays a novel and essential role in forming the Weibel-Palade bodies of endothelial cells. J Cell Biol 170, 627–636.
Mahoney MB *et al*. (2006). Presenilin-based genetic screens in *Drosophila melanogaster* identify novel notch pathway modifiers. Genetics 172, 2309–2324.
Marois E, Mahmoud A, Eaton S (2006). The endocytic pathway and formation of the Wingless morphogen gradient. Development 133, 307–317.
Metcalf DJ, Nightingale TD, Zenner HL, Lui-Roberts WW, Cutler DF (2008). Formation and function of Weibel-Palade bodies. J Cell Sci 121, 19–27.
Meyer C, Zizioli D, Lausmann S, Eskelinen EL, Hamann J, Saftig P, von Figura K, Schu P (2000). mu1A-adaptin-deficient mice: lethality, loss of AP-1 binding and rerouting of mannose 6-phosphate receptors. EMBO J 19, 2193–2203.
Miller SE, Collins BM, McCoy AJ, Robinson MS, Owen DJ (2007). A SNARE-adaptor interaction is a new mode of cargo recognition in clathrin-coated vesicles. Nature 450, 570–574.
Molinete M, Dupuis S, Brodsky FM, Halban PA (2001). Role of clathrin in the regulated secretory pathway of pancreatic beta-cells. J Cell Sci 114, 3059–3066.
Molinete M, Irminger JC, Tooze SA, Halban PA (2000). Trafficking/sorting and granule biogenesis in the beta-cell. Semin Cell Dev Biol 11, 243–251.
Morvan J, Tooze SA (2008). Discovery and progress in our understanding of the regulated secretory pathway in neuroendocrine cells. Histochem Cell Biol 129, 243–252.
Muskavitch MA, Hogness DS (1982). An expandable gene that encodes a *Drosophila* glue protein is not expressed in variants lacking remote upstream sequences. Cell 29, 1041–1051.
Niemeyer BA, Schwarz TL (2000). SNAP-24, a *Drosophila* SNAP-25 homologue on granule membranes, is a putative mediator of secretion and granule-granule fusion in salivary glands. J Cell Sci 113 (Pt 22), 4055–4064.
Orci L, Halban P, Amherdt M, Ravazzola M, Vassalli JD, Perrelet A (1984). A clathrin-coated, Golgi-related compartment of the insulin secreting cell accumulates proinsulin in the presence of monensin. Cell 39, 39–47.
Peden AA, Oorschot V, Hesser BA, Austin CD, Scheller RH, Klumperman J (2004). Localization of the AP-3 adaptor complex defines a novel endosomal exit site for lysosomal membrane proteins. J Cell Biol 164, 1065–1076.
Peden AA, Rudge RE, Lui WW, Robinson MS (2002). Assembly and function of AP-3 complexes in cells expressing mutant subunits. J Cell Biol 156, 327–336.
Peng YH, Yang WK, Lin WH, Lai TT, Chien CT (2009). Nak regulates Dlg basal localization in *Drosophila* salivary gland cells. Biochem Biophys Res Commun 382, 108–113.
Pirrotta V (1988). Vectors for P-mediated transformation in *Drosophila*. Biotechnology 10, 437–456.

Robinson MS (2004). Adaptable adaptors for coated vesicles. Trends Cell Biol 14, 167–174.
Roth GE, Wattler S, Bornschein H, Lehmann M, Korge G (1999). Structure and regulation of the salivary gland secretion protein gene *Sgs-1* of *Drosophila melanogaster*. Genetics 153, 753–762.
Shaner NC, Campbell RE, Steinbach PA, Giepmans BN, Palmer AE, Tsien RY (2004). Improved monomeric red, orange and yellow fluorescent proteins derived from *Discosoma* sp. red fluorescent protein. Nat Biotechnol 22, 1567–1572.
Sisson JC, Field C, Ventura R, Royou A, Sullivan W (2000). Lava lamp, a novel peripheral Golgi protein, is required for *Drosophila melanogaster* cellularization. J Cell Biol 151, 905–918.
Thomopoulos GN, Kastritis CD (1979). A comparative ultrastructural study of 'glue' production and secretion of the salivary glands in different species of the *Drosophila melanogaster* group. Dev Genes Evol 187, 329–354.
Thomopoulos GN, Neophytou EP, Alexiou M, Vadolas A, Limberi-Thomopoulos S, Derventzi A (1992). Structural and histochemical studies of Golgi complex differentiation in salivary gland cells during *Drosophila* development. J Cell Sci 102 (Pt 1), 169–184.
Tooze J, Tooze SA (1986). Clathrin-coated vesicular transport of secretory proteins during the formation of ACTH-containing secretory granules in AtT20 cells. J Cell Biol 103, 839–850.
Torii S, Saito N, Kawano A, Zhao S, Izumi T, Takeuchi T (2005). Cytoplasmic transport signal is involved in phogrin targeting and localization to secretory granules. Traffic 6, 1213–1224.
Waguri S, Dewitte F, Le Borgne R, Rouille Y, Uchiyama Y, Dubremetz JF, Hoflack B (2003). Visualization of TGN to endosome trafficking through fluorescently labeled MPR and AP-1 in living cells. Mol Biol Cell 14, 142–155.
Wasmeier C, Bright NA, Hutton JC (2002). The lumenal domain of the integral membrane protein phogrin mediates targeting to secretory granules. Traffic 3, 654–665.
Wasmeier C, Burgos PV, Trudeau T, Davidson HW, Hutton JC (2005). An extended tyrosine-targeting motif for endocytosis and recycling of the dense-core vesicle membrane protein phogrin. Traffic 6, 474–487.
Wingen C, Stumpges B, Hoch M, Behr M (2009). Expression and localization of clathrin heavy chain in *Drosophila melanogaster*. Gene Expr Patterns 9, 549–554.
Wucherpfennig T, Wilsch-Brauninger M, Gonzalez-Gaitan M (2003). Role of *Drosophila* Rab5 during endosomal trafficking at the synapse and evoked neurotransmitter release. J Cell Biol 161, 609–624.
Xu T, Rubin GM (1993). Analysis of genetic mosaics in developing and adult *Drosophila* tissues. Development 117, 1223–1237.
Zacharias DA, Violin JD, Newton AC, Tsien RY (2002). Partitioning of lipid-modified monomeric GFPs into membrane microdomains of live cells. Science 296, 913–916.